

Do environmental conditions determine whether salt driven decay leads to powdering or flaking in historic Reigate Stone masonry at the Tower of London?

Martin Michette^{a,*}, Heather Viles^a, Constantina Vlachou^b, Ian Angus^c

^a School of Geography and the Environment, University of Oxford, United Kingdom

^b Historic Royal Palaces, London, United Kingdom

^c Carden and Godfrey Architects, London, United Kingdom

ARTICLE INFO

Keywords:

Accelerated ageing
Architectural heritage
Conservation science
ECOS Runsalt
Ion chromatography

ABSTRACT

In order to evaluate the potential for using environmental controls as a preventive conservation strategy for Reigate Stone masonry, this paper tests the hypothesis that powdering and flaking decay patterns are a direct consequence of climatic variables. Samples of masonry affected by each decay pattern are analysed for soluble salt content using ion chromatography. The results are used to build thermodynamic models in ECOS Runsalt. These identify NaCl and NaNO₃ crystallisation in both environments, with NaCl dominating in powdering masonry and NaNO₃ dominating in flaking masonry. Freshly quarried samples of Reigate Stone with a range of physical characteristics are contaminated with a mixture of these salts. Replicates of each sample are subjected to two distinct accelerated ageing regimes. These regimes are based on environmental monitoring and designed to reproduce the observed decay pathways. One set is subject to partial immersion and relatively stable, high RH, to stimulate a zone of NaCl crystallisation near the surface. The replicate set is subject to occasional wetting and frequent drops in RH, to stimulate NaNO₃ crystallisation within the fabric of the stone. The results provide some indication that the intended decay mechanisms were achieved, supporting the hypothesis; however, physical variation in the stone was a far greater control on the rate of decay and the emergence of distinctive decay phenomena. This extended to both the mineralogical composition of the stone and to pre-existing decay features, such as crusts and cracks. The implication of these results is that the emergence of decay patterns in Reigate Stone cannot be explained solely by environmental mechanisms; baseline mineralogy and historical contingency can play a crucial role. Whilst environmental controls may provide a conservation strategy in some cases, it is likely that detailed assessment of the case specifics will be necessary.

1. Introduction

1.1. Background, aim and objectives

Salts are a major cause of deterioration in historic masonry (Charola, 2000). Predicting the dynamics of salt driven stone decay is a highly complex task, which requires carefully designed experimental frameworks (Flatt et al., 2017). Designing experimental procedures is complicated by the fact that rates and patterns of stone decay depend on interactions between petrophysical characteristics, type of salts, and environmental conditions (Menéndez and Petráňová, 2016; Yu and Oguchi, 2009). Computational tools such as ECOS Runsalt have been developed to assist with this complexity, but appropriate sampling

strategies are vital when linking experimental models to field data (Sawdy and Price, 2005a). Seasonal variations in salt concentration can present a further challenge when collecting field data (Sawdy and Price, 2005b). Building general theories from the discrete observations made in experimental data can overlook or exaggerate the effect of specific mechanisms or attributes (Sun and Zhang, 2019; McCabe et al., 2013; Warke and Smith, 2007). Theoretical predictions are frequently undone by practical observations, both in laboratory and field environments (Menéndez and Petráňová, 2016; Price, 2007). These factors combine to present significant challenges for the design of laboratory tests which reflect field behaviour (Lubelli et al., 2018); this in turn is an obstacle to developing conservation strategies for salt contaminated masonry.

The most highly valued building stones are often the most

* Corresponding author.

E-mail address: martin.michette@ouce.ox.ac.uk (M. Michette).

<https://doi.org/10.1016/j.enggeo.2022.106641>

Received 27 March 2020; Received in revised form 23 August 2021; Accepted 24 March 2022

Available online 4 April 2022

0013-7952/© 2022 The Authors. Published by Elsevier B.V. This is an open access article under the CC BY-NC-ND license (<http://creativecommons.org/licenses/by-nc-nd/4.0/>).

vulnerable: soft stones used for detailed carving at heritage sites, which have subsequently been exposed to centuries of weathering and use. Reigate Stone, an important freestone used widely in medieval London, frequently displays signs of salt contamination (Price, 1993). Neither a true sandstone or limestone, Reigate Stone is very fine grained and the main cementing component is opal-CT, although a variable calcite content can form an additional cement (Sanderson and Garner, 2001). Some Reigate Stone falls into the category of weakly cemented, alkaline, porous stone most susceptible to salt damage (Michette et al., 2020). Two distinctive, common stone decay patterns are frequently encountered in Reigate Stone (Vergès-Belmin, 2008) (Fig. 1):

1. A gradual powdering of the stone surface characterised by the continuous loss of material ranging in size from individual grains to millimetric agglomerations. Agglomerations tend to take the form of very fine plate like flakes with a thickness of only a few grains. Erosion can progress evenly or differentially. Differential erosion is particularly evident on stones which have a harder crust, which are still evident on many stones previously exposed to sulphation. In these cases, surface loss appears to gain a foothold in pits or perforations in the outer crust and progress locally; this can lead to alveolar formation.
2. A more episodic flaking characterised by periodic detachment of centimetric agglomerations. Agglomerations take a range of sizes but differentiate from those above in their greater thickness. In all but the most severe cases, agglomerations form plate like structures which appear to progressively delaminate from the surface. In some cases, these form fish-scale patterns. In some severe cases the stone breaks up into fragments irrespective of orientation. A series of

laminar flakes or scales may build up gradually before sub-surface detachment occurs and leads to significant material loss. In some cases, flaking appears to take place behind crusts or surface coats. This eventually leads to the catastrophic loss of the entire outer surface.

Both patterns are evident in more and less severe forms. Combinations of both decay patterns do exist, generally in very severe cases of decay in which they appear to be developing concurrently. Recently detached flakes can reveal a powdering sub-surface.

The precise mechanics that generate these different patterns are unclear; past studies have linked them to level of exposure (Sanderson and Garner, 2001; Lockwood, 1994); however, this is not a definite indicator. Although bedding planes can be faintly visible in Reigate Stone, cleavage does not appear to propagate parallel to bedding. Stones will flake and delaminate on two non-parallel external faces and in some cases will show evidence of delamination occurring parallel to mortar bedding at their edges (Fig. 1c). Different typologies of Reigate Stone were used throughout the medieval period, and the wide range of different environments and histories that extant masonry have been exposed to is likely to have resulted in highly varied salt contaminations (Michette et al., 2020; Michette et al., 2019; Price, 1993). Determining to what extent the controlling factors in these distinctive decay patterns are governed by the intrinsic properties of the stone, the nature of the contaminate, or the localised environment will inform the design of appropriate conservation strategies.

The main aim of this paper is to determine the role of environmental conditions on salt driven decay in Reigate Stone. This will assist the design of ongoing conservation strategies aimed at mitigating the effects

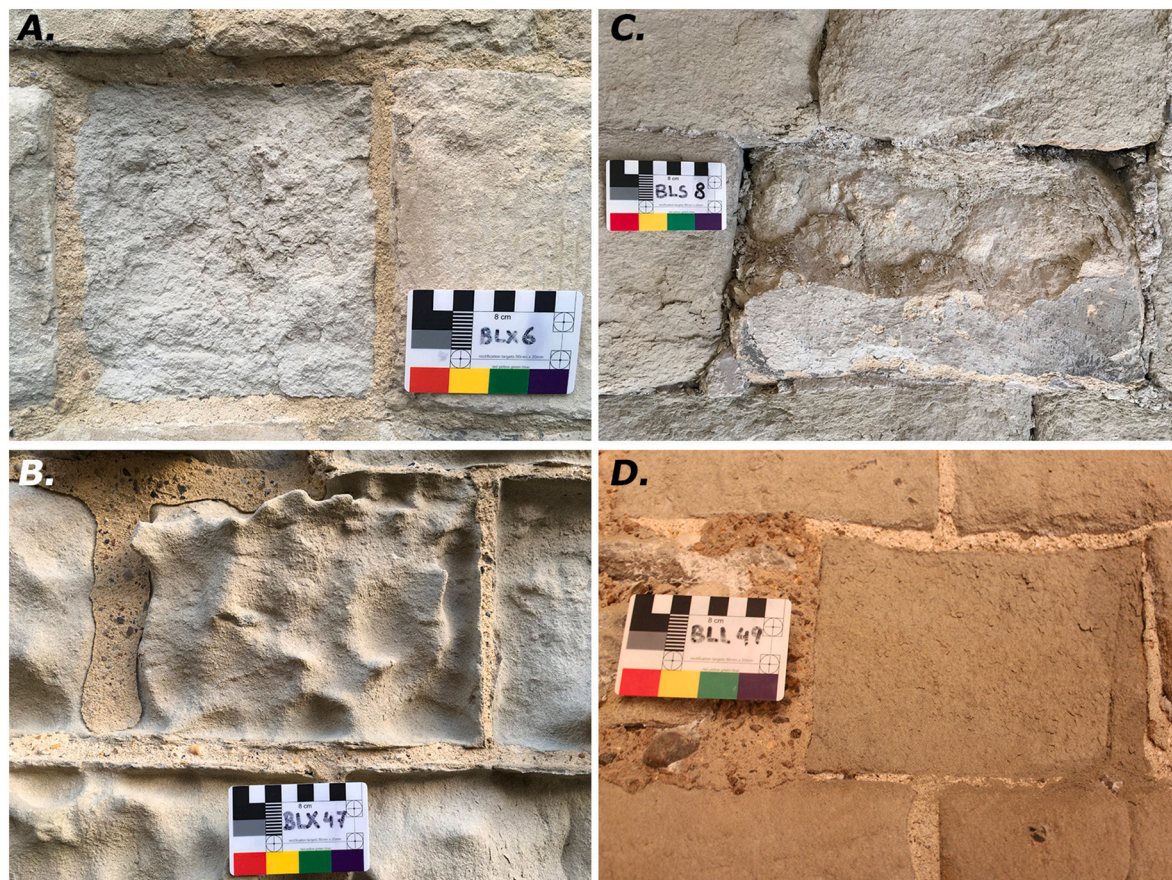


Fig. 1. Powdering and flaking Reigate Stone at the Bell Tower, Tower of London. A. Flaking stone in south-east facing external masonry; likely to represent 19th century repair material. B. Powdering stone in south-west facing masonry with alveolars; likely to represent primary medieval material. C. Flaking stone in stairwell, with delamination occurring parallel to front and side faces. D. Powdering stone in north-west alcove of lower chamber.

of salt driven decay. In particular, it will help determine whether interventive conservation procedures, aimed at improving petrophysical resistance, can be replaced by preventive measures, such as by maintaining safe relative humidity (RH) ranges for locations that display specific decay phenomena. In order to assess the relative role of environmental conditions, a secondary aim will be to determine the influence of petrophysical variability. The objective is to develop a methodology for laboratory experiments which reflect field behaviour that can be applied to Reigate Stone and other vulnerable historic building stones by:

- Determining typical compositions for salt solutions found in rapidly decaying Reigate masonry.
- Modelling a simplified mixture based on these typical compositions, designed to simulate salt dynamics found in-situ whilst eliminating salt variability as a factor.
- Simulating typical environments which appear to contribute to rapidly decaying Reigate masonry and subject a range of mineralogical typologies to accelerated ageing tests.

1.2. Reigate Stone decay at the Bell Tower, Tower of London

This study is part of a wider research project on Reigate Stone at the Tower of London. Michette et al. (2019) present a study of Reigate Stone decay at the Bell Tower, in which the decay patterns described above were associated with distinct environmental mechanisms. The Bell Tower is a two-storey, 12th century structure with a significant amount of surviving, primary Reigate masonry in a variety of settings and conditions. In-situ monitoring identified varying forms of flaking and powdering, corresponding to distinct locations and micro-climates inside the Bell Tower (Michette et al., 2019) (Fig. 2):

- Powdering dominates the lower chamber, ranging from gentle to severe. Differential erosion is noticeable in the west alcove, which has an open arrow slit. Erosion is severe yet regular in the north-west alcove, where the arrow slit has been covered.
- The upper chamber displays remarkably sound Reigate Stone with remnants of plaster and limewash. One noticeable exception is the southern alcove of the upper chamber, which contains severely powdering stones and combinations of severe powdering with flaking.
- Flaking dominates the spiral stair leading to the Bell Tower roof. This area is faced in fine Reigate ashlar, some of which is in a sound condition. Some of these stones are severely flaking. These are concentrated in but not limited to the west.

In the earlier study, these locations were monitored over an 18-month period in order to detect whether specific climatic variables are associated with these observable patterns of decay (Michette et al., 2019). The results suggested that powdering is related to deep wetting of the stone and a steady ambient climate; evaporation and salt crystallisation are taking place at or near the stone surface. Flaking is related to a dynamic moisture profile and seasonal and diurnal temperature cycles; salt crystallisation takes place beneath the stone surface. These results are compatible with a hypothesis that distinct environmental mechanisms govern the emergence of powdering and flaking decay phenomena in Reigate Stone, due to underlying differences in the dynamics of wetting and drying (Fig. 3). Similar hypotheses have been proposed by Lewin (1982), Colston et al. (2001), Lubelli et al. (2006), López-Arce et al. (2008) and Diaz Gonçalves and Brito (2014).

Decay patterns on the external masonry of the Bell Tower also can also be clearly subdivided according to flaking and powdering. Powdering dominates the west, north-west and north elevations. Flaking dominates the south-east, south and south-west elevations. Close inspection of the Reigate masonry indicates that the powdering and flaking stones belong to two separate mineralogical types (Michette

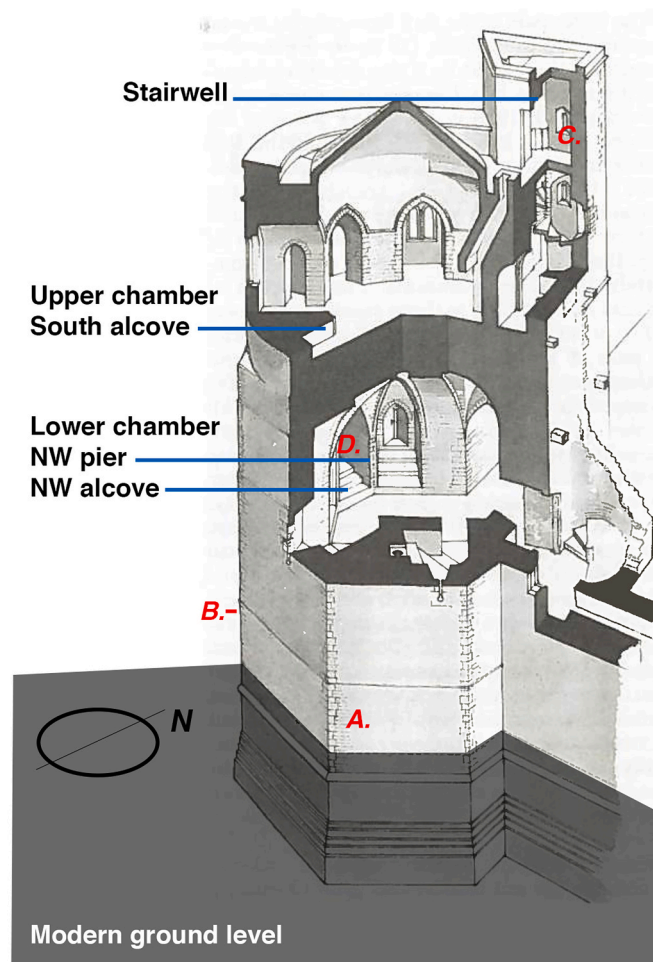


Fig. 2. Axonometric cut-away of the Bell Tower, Tower of London, highlighting areas of investigation in this study and showing approximate location of stones depicted in Fig. 1a-d. (original image by T. Bell).

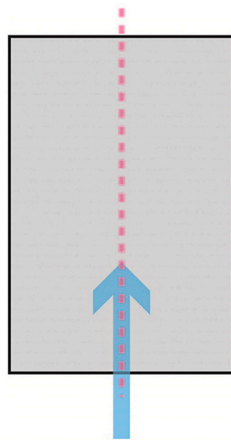
et al., 2020). The paler colour of the flaking stones suggests a higher calcite content; the greenish, grey hue of the powdering stones suggests a higher clay content (Fig. 1). It is likely that the south facing Reigate masonry represents 19th century repair work. Whilst a variety of environmental mechanisms may be contributing to decay in different orientations of external masonry, these observations imply that the emergence of decay patterns is governed by petrophysical characteristics.

The Bell Tower therefore present two contradictory explanations for the emergence of distinctive flaking or powdering decay patterns. Environmental monitoring provides evidence in support of a hypothesis on separate hygro-physical mechanisms leading to divergent decay pathways; however, observations of more widespread occurrence of the resulting decay patterns indicate that underlying petrophysical characteristics may also explain variation.

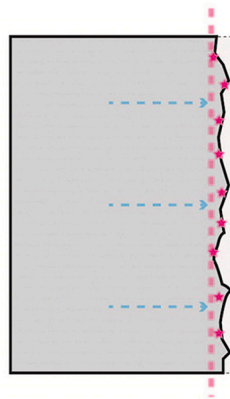
1.3. Salt decay in historic masonry

Salt driven decay is intrinsically linked to moisture transport. Advection and diffusion are responsible for the distribution of salts within a porous matrix (Flatt et al., 2017). During wetting, moisture from the environment can cause salt crystals to deliquesce; capillary forces and/or differences in vapour pressure will cause the subsequent solution to migrate through the porous network (Lieberink et al., 2018). During drying and given suitable thermodynamic conditions determined by equilibrium RH, salts will re-crystallise. The zone of crystallisation

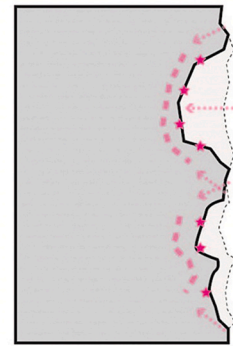
Powdering



Constant moisture ingress leads to deep wetting.

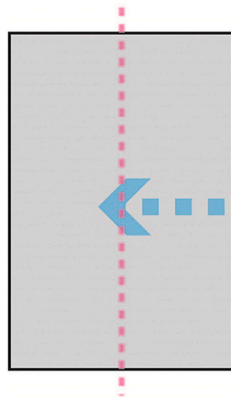


Fixed zone of salt crystallisation at stone surface.

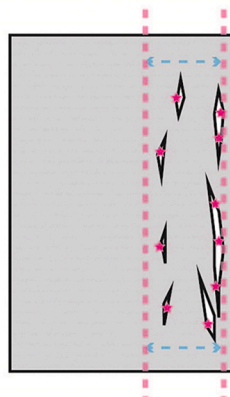


External conditions determine rate and pattern of decay.

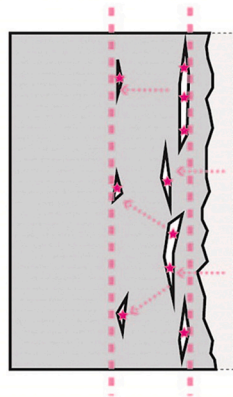
Flaking



Variable moisture ingress leads to uneven distribution.



Mobile zone of salt crystallisation beneath surface.



Surface collapse begins new cycle of decay.

Fig. 3. Diagrammatic description of hypothetical mechanics underlying powdering and flaking decay patterns.

can be related to the drying phase. If moisture is evaporating from the surface of the material (drying phase 1), this can result in efflorescence (crystallisation at the outer surface). If environmental conditions can no longer maintain an evaporation front at the surface of a material (drying phase 2), this can result in subflorescence (crystallisation beneath the surface) (Modestou et al., 2015). The resulting crystallisation pressures can result in damage to the building stone and drive surface loss.

Colston et al. (2001) highlight the influence of drying phases in an investigation of decaying limestone piers inside a church in Norfolk. An area of deterioration starting at a height of approximately 2.5 m corresponds with an area of historic sodium chloride (NaCl) contamination. The area is too high to be affected by capillary rise and the moisture content is shown to be in balance with atmospheric humidity. Under these conditions, adsorbed atmospheric moisture cannot re-supply evaporation at the stone surface during drying phases; suitable thermodynamic conditions will result in crystallisation cycles taking place

below the surface of the material, leading to the observed decay pattern. The lower part of the piers is strongly affected by capillary rise. Due to the constant supply of moisture, evaporation occurs at the surface and the salt solution is emitted from the fabric.

Petrophysical characteristics that play an important role in salt driven decay can be divided into two groups (Flatt et al., 2017). The first group covers properties affecting the accumulation of salts. These include the chemical composition of the stone, principally the presence of alkali anions, which will determine whether salts can be formed in-situ in reaction to cationic contamination. They also include pore space open to capillary flow, which enables rapid moisture uptake (Yu and Oguchi, 2009). The second group covers properties affecting the resistance to salt decay mechanisms. These include the strength and anisotropy of the rock (Benavente et al., 2007a); tensile strength is the key determiner, however a good correlation to compressive strength has been determined. They also include porosity susceptible to

crystallisation pressures; generally, this covers the micro-porous region (Benavente et al., 2007b). Combining these factors indicates that weakly cemented, alkaline stones with a high, bimodal porosity are likely to be the most susceptible to salt damage.

The shape and size of pores can further influence salt driven decay. Accelerated ageing tests were used to determine that large pores and fissures act as a sink to consume high supersaturation (Benavente et al., 2007b). On the other hand, narrow fissures were found to be particularly susceptible to the crystallisation pressures generated by salt. Ongoing crystallisation cycles caused these to coalesce and form larger fissures. The study also found that a high porosity, low pore-radius, weak strength matrix could be linked to granular disintegration. Liefferink et al. (2018) found that during deliquescence of NaCl in porous media, the invasion of salt solution is controlled by capillary pressure within the porous network. In hydrophilic media, the liquid formed by deliquescence preferentially invades adjacent small pores and migrates towards higher vapour pressure. Repeat wetting and drying cycles can thereby cause a progressive expansion of porous matrix, which could generate near surface flaking. These findings begin to associate specific decay pathways with distinct pore network characteristics.

The nature of the salt contamination influences the onset and pattern of crystallisation and resultant decay pathways. Under equal conditions, different salts will crystallise at different depths or heights as a function of their solubility (Arnold, 1982). Different salts have been shown to produce different decay rates and patterns in stones (Yu and Oguchi, 2009). However, whilst certain salts are shown to be highly aggressive across numerous studies, rates and patterns vary from stone to stone and it is not possible to construct clear categories based on the efficacy of salts (Lubelli et al., 2018). Mixed salt solutions complicate matters further and may be more, or less aggressive than single salts depending on their composition (Menéndez and Petráňová, 2016; López-Arce et al., 2008); recent studies have emphasised the importance of testing procedures using mixed salt solutions to better reflect scenarios encountered in historic masonry (Lubelli et al., 2018).

These complex synergies make generalised associations between agents and pathways of decay impossible (Charola, 2000). However, in individual cases it has been possible to correlate decay patterns with specific types of salt contamination or environmental conditions. Using an accelerated ageing test to compare the effects of pure magnesium sulfate (MgSO_4) with a salt mixture, López-Arce et al. (2008) were able to reproduce the characteristic flaking of a Magnesian limestone church in York. Pel et al. (2019) were able to describe decay functions for situations in which a sandstone has a continuous flux of NaCl solution from a moisture source (i.e. advection due to ground water) to a surface exposed to evaporation. Rodríguez-Navarro and Doehne (1999) were able to associate sodium sulfate (Na_2SO_4) and NaCl damage with the location of crystallisation, which itself was determined by evaporation rates. Associating decay patterns with the underlying dynamics can be an effective diagnostic tool, and an important step in the design of preventive conservation strategies aimed at controlling specific environmental mechanisms.

2. Methodology and results

2.1. Overview

A three-step methodology is used to address the objective of developing an experimental framework that reflects field behaviour. The aim is to stimulate flaking and powdering decay phenomena observed in Reigate Stone at various locations around the Bell Tower, Tower of London.

Step 1. Masonry exposed to the micro-environments monitored in Michette et al. (2019) is sampled and analysed using ion chromatography. Distinct, complex, ionic mixtures are found in each

area of the Bell Tower, with some seasonal variation also present.

Step 2. The ionic concentrations are modelled in ECOS Runsalt to determine which salts are at risk of crystallisation cycles under climatic conditions measured in Michette et al. (2019). A simplified salt mixture is modelled by isolating salts at risk of crystallisation in both the lower chamber and stairwell environments (Fig. 2).

Step 3. Ten specimens of Reigate Stone, representing different mineralogical types examined in Michette et al. (2020), are contaminated with a highly concentrated mixture of NaCl and sodium nitrate (NaNO_3). This includes stone from quarries believed to have supplied building material during the construction and repair phases of the Bell Tower (Burgess, 2008). Replicates of each specimen are exposed to two distinct accelerated ageing regimes, designed to simulate the environmental mechanisms identified in Michette et al. (2019) and described in Fig. 3.

In the following section each step is described sequentially. As the results of one methodological step inform the design of the following step, these descriptions include both a detailed explanation of the experimental method and an outline of the results.

2.2. Ion chromatography

2.2.1. Method

Samples of Reigate Stone were collected from three distinct micro-environments in the Bell Tower for determination of soluble salt content. As well as from the lower chamber and stairwell environments, characterised by powdering and flaking surfaces respectively and monitored in Michette et al. (2019), material was gathered from powdering surfaces in the upper chamber.

Powdering material was gathered in dust trays placed at the foot of rapidly decaying masonry. To enable an investigation of spatial distribution, dust trays were placed at two different locations in the lower chamber (Fig. 2). One dust tray was placed in the south alcove of the upper chamber. To enable an investigation of changes in seasonal distribution, material gathered in dust trays was collected at bi-monthly intervals for laboratory analysis. Following episodic detachment of surface flakes in the stairwell, small flakes were collected for laboratory analysis.

Collected material was analysed using liquid ion chromatography (Dionex). Samples were ground to a fine powder. 1 g of each sample was added to 50 ml of deionised water, agitated, sonicated and filtered to produce solution. The solution was appropriately diluted (x10 or x100) following conductivity testing to keep the results of Dionex analysis within standards range.

2.2.2. Results

Fig. 4 shows the concentration of soluble anions and cations present in the samples in parts per million. Sodium, potassium, magnesium and calcium cations, and chloride, nitrate and sulphate anions are present to varying degrees in all samples. The overall concentration of ions is high in all samples, even when compared to previously measured salt content in Reigate Stone at the Tower of London (Church, 2003). In material collected from the lower and upper chamber, detached dust sampled from powdering surfaces is likely to contain a disproportionately high amount of salt. The concentrations measured in flake samples collected from the stairwell are more comparable to previous results. Material sampled from the upper chamber is dominated by sulphate and calcium ions. Due to the likely dominance of insoluble gypsum, these samples were not considered in the ongoing thermodynamic modelling. The lower chamber samples are dominated by sodium and chloride ions, with notable variation in seasonal and spatial distribution. Stairwell samples have a high concentration of nitrate ions.

In the lower chamber, the overall concentration of salts decreases in

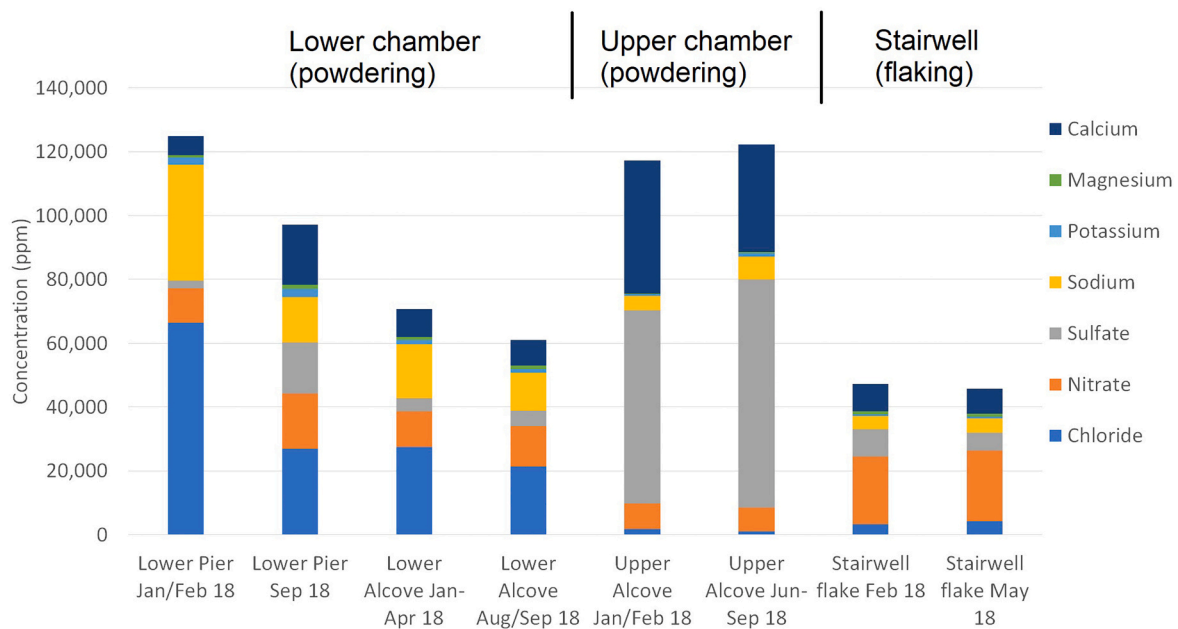


Fig. 4. The concentration of soluble ions varies during different sampling periods and in different areas of the Bell Tower, Tower of London.

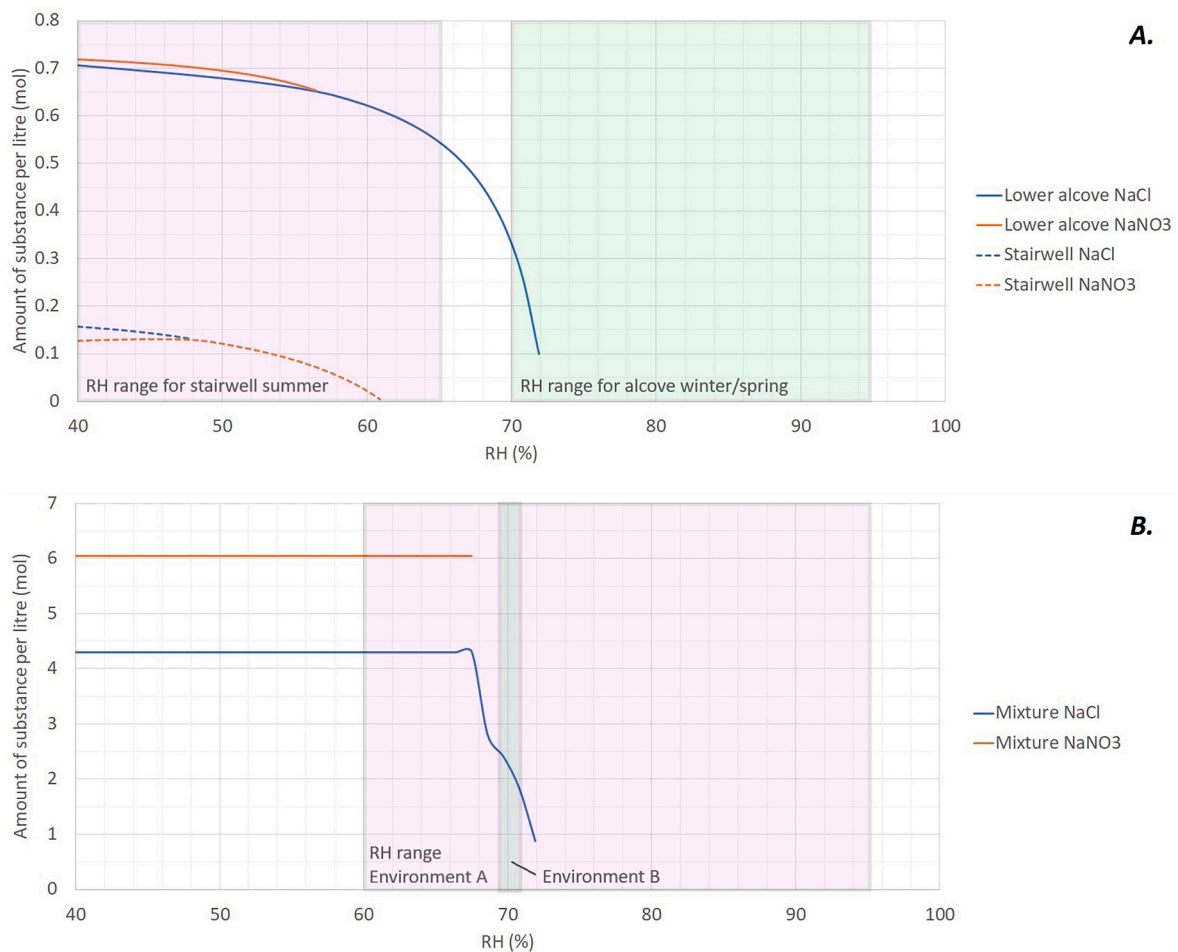


Fig. 5. A. Runsalt models based on ionic concentrations measured in the lower chamber alcove (Jan-Feb sample) and the stairwell (May sample). Relative humidity (RH) ranges established in Michette et al. (2019) are superimposed. Temperature set to 10 °C for lower chamber and 25 °C for the stairwell. B. Final iteration of Runsalt model developed to represent crystallisation scenarios in both lower chamber and stairwell environments using simplified, unified salt mixture of 250 g NaCl and 150 g NaNO₃ per litre of water. Temperature in model set to 15 °C. RH range for proposed accelerated ageing regimes superimposed.

summer months. This decrease correlates with an increase in detaching material, particularly in material collected from the pier (Michette et al., 2019). The increase in detaching stone can also explain the increase in gypsum and calcite implied by the redistribution of ionic concentration. There is also a notable increase in the relative amount of nitrate in material collected from the lower chamber during summer months. In the upper chamber, where the rate of detachment was steadier throughout the year, and in the stairwell, where detachment was episodic, there is less seasonal variation in concentration.

2.3. Thermodynamic modelling

2.3.1. Method and results

For each sample from the lower chamber and stairwell environments, the measured ionic concentrations were entered in to Runsalt in order to model salt solutions and potential crystallisation/ deliquescence scenarios. Runsalt is a graphical interface to the ECOS (Environmental Control of Salts) thermodynamic model developed by Price (2000), which predicts the crystallisation and deliquescence points of salt crystals in complex solutions of mixed salts under dynamic temperature or RH (Bionda, 2005). An option to automatically remove gypsum from the simulation was selected; as gypsum solubility is very low, ions bound in gypsum are unlikely to contribute to dynamic crystallisation and deliquescence. Temperatures for each environment were set to mean values measured in Michette et al. (2019), in order to assess the effect of changes in RH and identify which salts were at risk of crystallisation.

The autobalance option was used to correct minor discrepancies in the molecular balance of the analysed solutions. In case of larger discrepancies, the concentration was manually balanced by reducing calcium content to account for the presence of calcite in the samples. This is similar to the approach used by Price (2007). In most models there was no difference between selecting autobalance and manually balancing calcium content; in models of the lower alcove the manual balance slightly increased the amount of NaNO_3 crystallisation.

Fig. 5a shows a selection of the Runsalt models, plotting the amount of crystallising salt in response to changes in RH given the ionic compositions measured at various locations. In models of the lower chamber, a risk of NaCl crystallisation was identified in every location and throughout the year, although the risk is low in winter months. Of other potential compounds within the ionic compositions, only NaNO_3 is at risk of crystallisation under the conditions measured by Michette et al. (2019). This risk is restricted to the alcove locations, and conditions for crystallisation are more favourable in summer months, although the ionic composition is more favourable for NaNO_3 in winter months. The results suggest it is highly likely that near surface NaCl crystallisation is the main cause of powdering in these locations. A risk of NaCl crystallisation was also identified in models of the stairwell, particularly in summer months when RH falls below 50% for long periods of time. However, NaNO_3 crystallisation is more common here and likely to take place when RH falls below 60%, which happens in spring, summer and autumn months.

A unified model was built based on salts at risk of crystallisation in both environments (Fig. 5b). This was used to design a representative salt mixture for use in the accelerated ageing experiment. The model was based on a mixture of NaCl and NaNO_3 . Iterations identified a mixing proportion of 10 sodium ions to 7 chloride ions to 3 nitrate ions as providing a solution which would form NaCl crystallisation throughout the year under conditions monitored in the lower chamber, with some risk of NaNO_3 crystallisation in summer months. The more pronounced swings in RH monitored in spring, summer and autumn months in the stairwell would result in multiple NaNO_3 crystallisation cycles, although it should be noted that the order of crystallisation is reversed from that predicted in the stairwell models.

2.4. Accelerated ageing

2.4.1. Method

Fig. 6 provides a diagrammatic overview of the final methodological step, which aimed to reproduce the decay phenomena observed in Michette et al. (2019) under controlled environmental conditions. Reigate Stone samples were contaminated with a mixed salt solution and subjected to accelerated ageing regimes designed to simulate the environmental decay mechanisms identified by Michette et al. (2019). The samples were selected from material which had been extracted from quarries in a project coordinated by Historic Royal Palaces in 1999 and analysed by Michette et al. (2020). Ten specimens were selected from four different, historic quarries (Sowan, 1975). Petrophysical characteristics, such as mineralogical composition, porosity and strength, varied across and within the individual quarries (Table 1). Quarry RS is known to have supplied medieval building works; quarry QF is known to have supplied 19th century building and repair works (Burgess, 2008). Samples from quarry GA show remarkable physical diversity within a single working face; samples from quarry GO are more homogeneous (Michette et al., 2020). Each specimen was divided in to two 4.5 cm diameter x 4.5 cm high cylindrical replicates. Replicates were prefixed according to quarry, numbered, and then suffixed according to the accelerated ageing environment they were exposed to.

A highly concentrated solution was prepared based on the results of the thermodynamic modelling, consisting of 250 g NaCl and 150 g NaNO_3 per litre of deionised water (Fig. 5b). These measurements were chosen to provide an easily reproducible recipe and a mixture which was not fully saturated. Full saturation was avoided to minimise viscosity and likelihood of pore clogging (Lubelli et al., 2018). Replicates from each specimen were then subjected to two separate accelerated ageing tests as detailed in Fig. 6 and below. Loose and detached material was collected from the samples at intervals, and dried, weighed, sorted by grain size and photographed to determine the nature of material (salt or stone) and the size of the largest detached fragment. Sorting was done using 1 mm and 0.25 mm sieves, with care taken not to break down detached grains further during sieving. The samples were also regularly photographed to document surface change.

2.4.1.1. Preparation and calibration.

1. Dried at 60 °C until mass equilibrium.
2. Submerged in the salt solution until mass equilibrium.
3. Dried at 60 °C until approaching mass equilibrium (<1% change over 12-h period) in order to determine the amount of absorbed salt (Table 1).
4. Replicates from each specimen placed in different simulated environments (henceforth Environments A and B).

2.4.1.2. Environment A. Simulated in a Binder climate chamber. Conditions were programmed to cycle between an 18-h period at 95% RH and 10 °C, and a 6-h period at 60% RH and 25 °C for a total of 10 weeks, with a repeat full immersion after 5 weeks. This environment was chosen to stimulate rapid, sub-surface NaCl and NaNO_3 crystallisation, and simulate the Bell Tower stairwell, which was dominated by flaking. Loose material was brushed off the samples using a stiff brush and collected after weeks 1, 5, 6 and 10.

2.4.1.3. Environment B. Simulated in a Weiss climate chamber, with brief periods in a Sanyo and a Binder climate chamber due to technical issues. The samples were subjected to a first phase of continuous partial immersion, and a second phase of repeated partial immersion, each time placed in stable environment of 70% RH and 15 °C for 6 weeks. This

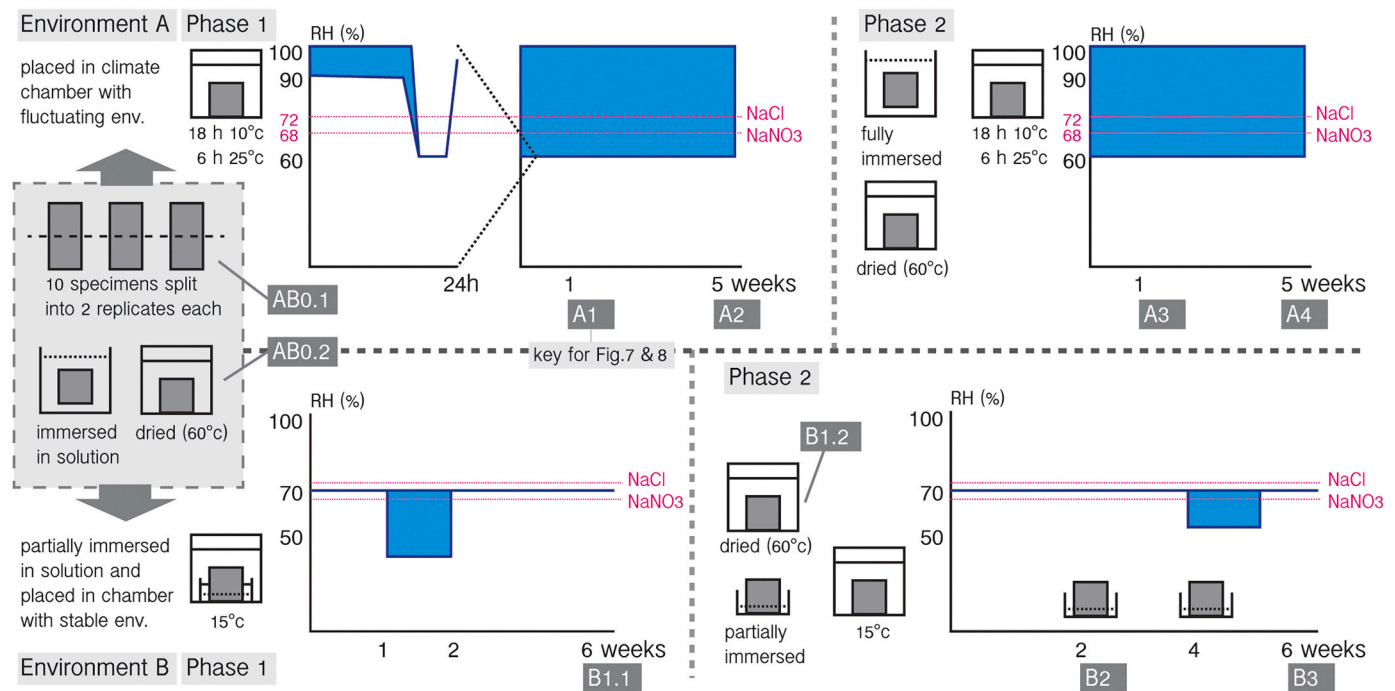


Fig. 6. Diagrammatic overview of accelerated ageing regimes showing sample preparation steps and separate climate chamber programmes for two sets of replicates. NaCl and NaNO₃ crystallisation/ deliquescence relative humidity marked by pink dotted line. Sequential photo numbering system used in main text and Figs. 7 & 8 shown in dark grey boxes. (For interpretation of the references to colour in this figure legend, the reader is referred to the web version of this article.)

Table 1

Salt uptake, total loss, and type and size of largest lost piece from each replicate of every specimen in response to different accelerated ageing regimes.

Specimen	Calcite content (%) ^a	Clay content (%) ^a	Porosity (%) ^a	Env. A salt uptake 1 (g)	Env. A salt uptake 2 (g)	Env. A total loss (g)	Env. A largest loss (mm)	Env. A largest loss type	Env. B salt uptake 1 (g) ^b	Env. B loss (g)	Env. B largest loss (mm)	Env. B largest loss type
GA1	28	6	27.6	12.4	0.6	2.03	15	Salt crust	11.8	0.3	3	Salt crystal
GA2	9	25	35	9.1	2.6	18.01	20	Stone flake	10.8	17.98	25	Stone flake
QF1	14	42	33.7	14.8	3.8	0.42	10	Salt crust	11.8	0.3	4	Salt crystal
QF2	19	8	34.5	14.6	2.3	0.69	18	Salt crust	14.5	0.37	4	Salt crystal
RS1	12	10	33.9	13	2.9	1.64	15	Salt crust	11.5	0.45	5	Salt crystal
RS2	18	6	33.9	13.9	3.1	0.34	12	Salt crust	12.1	0.33	5	Salt crystal
RS3	16	22	35.2	15.2	3.7	1.08	12	Salt crust	12.7	0.21	3	Salt crystal
GO1 ^c	15	17	36.1	13.3	3.1	1.56	25	Salt crust	–	–	–	–
GO2	17	14	35.4	12.8	4.7	6.7	30	Stone flake	11.3	0.46	4	Salt crystal
GO3 ^c	16	18	38.6	–	–	–	–	–	14.7	0.36	17	Stone flake

^a Material characteristics taken from Michette et al., 2020.

^b Additional salt uptake in environment B occurred during continuous and repeat partial immersion.

^c No loss recorded in control samples.

setup was designed to stimulate gradual NaCl crystallisation at the outer surface (although technical issues resulted in occasional drops into the NaNO₃ crystallisation range), and simulate the lower Bell Tower, which was dominated by powdering. Loose material was brushed off and collected after weeks 6, 8, 10 and 12.

For phase 1, the samples were placed in individual containers so that the bottom 1 cm was sealed, and the bottom 0.5 cm was in contact with approx. 0.5 ml of salt solution. Top 3–3.5 cm of the sample exposed. For phase 2, samples were partially immersed outside the cabinet in 0.5 ml of salt solution until the solution had been fully absorbed, and then

replaced without individual containers. Partial immersion and replacement in the cabinet was repeated twice. During both phases, there were periodic, localised variations in RH and temperature due to technical issues, with RH dropping into the NaNO₃ crystallisation range for up to a week (Fig. 6). During the first phase, these drops in RH were not evenly distributed around the climate chamber and affected some samples more strongly than others.

2.4.1.4. Controls. Uncontaminated replicates of GO1 and GO3 were placed in the same environment as their contaminated replicates, one

sample in each environment, to provide a control. The control samples were immersed in de-ionised water under at the same times and using the same procedure as their contaminated replicates were immersed in solution. The small number of control samples reflects the lack of working quarries and the limited availability of Reigate Stone; the control set was built from the more homogeneous GO samples.

2.4.2. Results

Fig. 7 shows the weight loss and grain size distribution of individual samples following the successive cycles of the accelerated ageing. Fig. 8 shows photographs taken of a representative selection of samples at various stages of the experiment. The same stages are not shown for each

sample. Instead, a selection was made in order to best describe the various observed decay phenomena. Table 1 shows total weight loss for each replicate of all samples, with additional data on petrophysical characteristics taken from Michette et al. (2020). The samples responded differently to the two accelerated ageing regimes. Surface loss commenced in most samples subjected to the fluctuating RH of environment A after less than 1 week. Efflorescence formed on some samples during the continuous partial immersion phase of environment B, but only GA2 experienced surface loss. Besides efflorescence, some samples experienced surface loss during the repeat partial immersion phase of environment B. There was no loss or surface change recorded in the control samples, indicating that all measurable decay was in response to

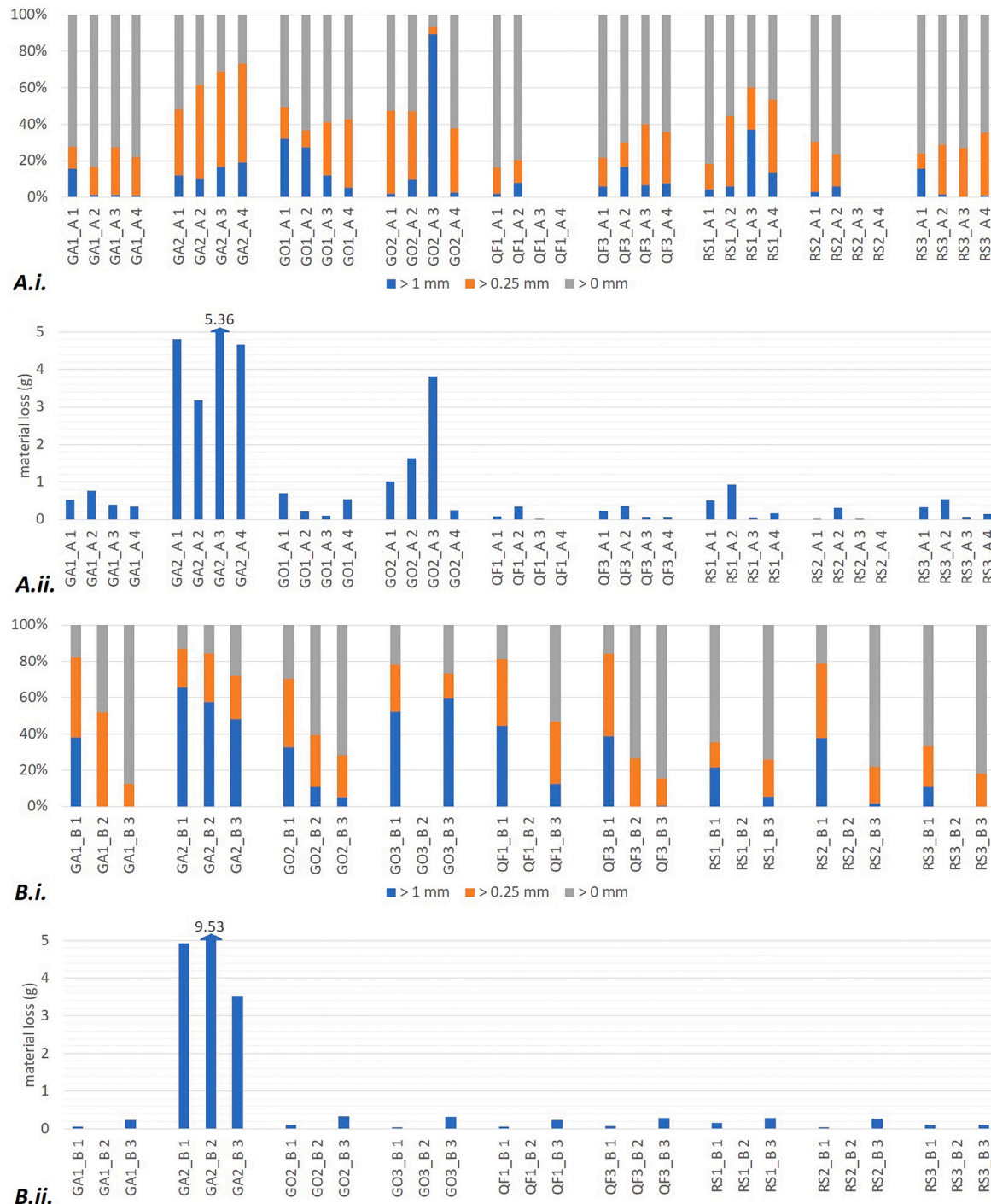


Fig. 7. Grain size distribution (i.) and total loss, including salt, (ii.) at different stages of accelerated ageing regimes for environments A and B.



Fig. 8. Three stages of decay in selection of samples exposed to environments A and B. Referencing system in Fig. 6 explains timing of photos. Rate and pattern of decay in both environments is strongly dependent on quarry provenance and individual stone characteristics. Loss of larger pieces of material usually related to pre-existing structural flaws (e.g. GO2_A and GA2_B), but some phenomena reminiscent of flaking seen in response to environment A (e.g. GA2_A and intermediate stages of QF1_A & RS1_A). Rate and homogeneity of surface decay in response to phase 2 of environment B strongly dependent on formation of salt crust during phase 1.

the salt contamination.

The initial and intermediate drying of samples was performed in order to calibrate the response to the distinct ageing environments. The initial drying of samples prior to placement in accelerated ageing environments resulted in a thin crust formation. This rapidly detached in environment A, with the largest detaching piece in most samples consisting of films of salt crust lost during the first phase of RH fluctuations. In environment B, the crust did not detach during the continuous partial immersion phase and was still evident during the intermediate drying prior to the second phase of ageing. In GA2, cracks appeared in the crust during the intermediate drying. Following the subsequent round of wetting and placement in the cabinet at stable RH, this resulted in an explosive loss of surface material. It is likely that the effect of these drying phases on the decay of the samples was at least as significant as the more long-term environmental simulations.

Environment A resulted in differential rates of material loss. These appear to be loosely governed by petrophysical characteristics, such as calcite and clay content and porosity, which can be linked to strength and hygric performance (Michette et al., 2020). There are no immediately clear patterns, with the most argillaceous samples (QF1) losing

only a small amount of material, and the most calcareous samples (GA1) losing a relatively large amount of material. Following the detachment of the outer salt crust formed during initial drying, the general pattern of decay in samples exposed to environment A more strongly resembles forms of severe powdering found on Reigate Stone in historic masonry. Only in GA2 did the general pattern of decay resemble the flaking encountered in historic masonry. This sample represents a high clay, low calcite typology, which is unlikely to be representative of extant building stone (Michette et al., 2020; Sanderson and Garner, 2001). During the second phase of humidity cycling, a large fragment of GO2 detached along a pre-existing structural fault. These observations give some indication that environment A was driving a decay mechanisms which broadly supports the hypothesis being tested, with frequent, high amplitude cycles in RH driving subflorescence, deliquescence and redistribution of salts; however, the pathways and rates of decay, and the emergence of distinct patterns, was more strongly linked to structural idiosyncrasies.

In environment B, samples remained fully saturated throughout the continuous partial immersion phase. The amount of efflorescence was strongly dependant on the location of the samples in response to

uncontrolled drops in RH; it was highest in GA1, which was closest to the source of the uncontrolled fall in RH. During this phase, a thick salt crust built up in some samples (e.g. GA2 and RS3). The presence of this crust strongly influenced ongoing decay during the second phase of environment B. During the repeat partial immersion phase, the samples were able to begin drying when replaced in the cabinet. This resulted in some surface loss. Surface loss on all but two samples placed in environment B was limited to small amounts of granular disintegration. In many samples, the majority of recorded loss during the second phase was in the form of salt crystals, with no significant loss of stone surface. The grain size distribution of material loss in environment B is strongly affected by the formation of these millimetric salt crystals. The pattern of ongoing efflorescence was strongly dependent on the formation of a crust during continuous partial immersion. Samples in which a thicker crust formed (e.g. RS3) were prone to differential ongoing decay. Samples in which there was little efflorescence or crust during continuous immersion (e.g. QF3) decayed more homogeneously during the second phase. Following the final repeat partial immersion and drying cycle, during which RH fell to 55% for 1 week, there was noticeably more material loss in most samples, including more granular disintegration. The salt crust also began to blister. One larger stone flake detached from the edge of G03 during this cycle. As with environment A, there were signs that a specific mechanism was being achieved, in this case surface evaporation and near surface crystallisation in response to ambient climate; however, this did not result in the emergence of a specific decay pattern, with pathways strongly dependant on the particularities of the individual samples.

3. Discussion

The results of this study indicate that incidents of powdering and flaking decay in the masonry of the Bell Tower cannot be fully reproduced on the basis of environmental controls alone. This echoes findings made in other studies which aimed to unpick the relevant weighting of stone type, salt type and environment in salt driven decay processes. Menéndez and Petráňová (2016) were unable to make clear correlations between the decay caused by mixed salt solutions on different lithotypes subjected to different environmental mechanisms. Yu and Oguchi (2009) suspected that individual stone-salt interactions could be a key control in diverging decay pathways. Whilst López-Arce et al. (2008) were able to reproduce observed decay patterns in historic masonry using a methodological approach similar to the one presented in this study, their findings also highlighted the importance of reproducing accurate salt contamination and using comparable stone types in accelerated ageing tests. There was a strong reliance on relevant baseline data in the interpretation of results from these studies which is mirrored in this study. Given these specific factors, findings may be of limited use to a generalised model of stone driven decay. However, a step-by-step methodological approach which establishes laboratory conditions based on field data may be a useful framework for standardising future tests (Lubelli et al., 2018). Understanding limitations to methodologies such as the one presented here will help the ongoing development of such a framework.

The nature of salt crystallisation stimulated by the accelerated ageing regimes is likely to have been a key cause of deviation in the reproduced decay phenomena. The mixture used in this study was based on a simplified interpretation of measured ionic compositions from two environments. Differences in concentration and composition will have affected wetting and drying cycles and are likely to have influenced the emergence of decay patterns. The morphology of crystal formation can influence ongoing evaporation. Both theoretical and experimental evidence has shown that crust formation can reduce evaporation whereas patchy efflorescence can enhance evaporation (Veran-Tissoires and Prat, 2014; Eloukabi et al., 2013). The high concentration of the mixture used in this study and complete saturation of the samples are likely to have resulted in a clogging of the pores during the gradual evaporation of

samples in environment B (Espinosa-Marzal and Scherer, 2013; Rossi-Manaresi and Tucci, 1991). This 'crust formation' inhibited ongoing surface evaporation, both while the samples were in the climate chamber and during the intermediate drying. In the most extreme case of GA2_B, this resulted in a catastrophic flaking episode as subsurface decay caused the crust to collapse. In environment A, the order of crystallisation was reversed, with ECOS Runsalt predicting NaNO₃ crystallisation prior to NaCl crystallisation based on the sampling. The order in which salts precipitate out of a mixed solution should be taken into account (Charola, 2000). The experimental methodology used in this study was designed to eliminate the potential variability of diverging decay pathways due to differences in salt contamination; the findings indicate that this approach cannot fully explain field behaviour. Different contaminating solutions can result in similar patterns, for example in the powdering upper and lower chambers of the Bell Tower, and single salts can induce both flaking and powdering depending on environmental conditions (Amadori et al., 1989). However, unifying complex solutions in order to recreate dissimilar patterns may have excluded crucial components of the underlying chemistry.

The thermodynamic models produced here also expose some contradictions within the overall hypothesis of environmentally driven decay. The ionic concentrations measured in powdering samples from the lower chamber are representative of detached material, but not necessarily of the overall composition within the masonry. Composition is likely to be skewed towards salts which have crystallised near to the surface and detached along with powdering stone (Sawdy and Price, 2005a). However, despite the noticeable seasonal change in measured ionic composition of material collected from the pier, ECOS Runsalt predicts only NaCl crystallisation in both winter months and summer months. This indicates either the introduction of new contaminants throughout the year, or a significant redistribution of salt concentration within the masonry across the year, or it suggests decay mechanisms which are not explained by the crystallisation scenarios predicted in Runsalt, such as additional crystallisation or phase change activity, hygric swelling of clay, or thermal activity. There are similar contradictions exposed by the flaking episodes during winter months observed in Michette et al. (2019), at times when RH is unlikely to have dropped within the range predicted to result in crystallisation by Runsalt. The proximity to a wooden spiral staircase and the vibrations and abrasions this causes is likely to represent an additional cause of detaching material. Whilst the hypothesis tested here can explain the general direction of decay pathways, contradictions within the model imply that there are additional environmental and contextual factors which contribute significantly to the phenomenology and pattern of decay.

Further constraints to the methodology exist within the limitations of accelerated ageing in climate chambers, and the upscaling of phenomena recorded in experiments to identify corresponding patterns in historic masonry (Hall et al., 2012). The use of cylindrical cores reduces some of the edge phenomena often encountered with small, rectangular samples in accelerated ageing tests (Lubelli et al., 2018). However, the geometry of the samples is fundamentally different from the historic masonry in the Bell Tower. This will be reflected in the shape and scale of moisture transport dynamics. Dry weight loss does not always provide a good indication of decay taking place within a porous network. Wave-length velocity has been proposed as an alternative or complementary indicator (Benavente et al., 2007b). Limitations to this technique were encountered in this study relating to the comparison of measurements at different stages of the experiment, and the influence of any additional drying or wetting to make the samples more comparable. The grain size distribution approach adopted from Goudie (1986) provides a useful additional metric, but care must be taken to differentiate detached stone from salt. Ongoing work can include a destructive analysis of the samples and a comparison of pore structure with comparative samples that have not been aged.

Past studies have associated pore-size distribution and other physical characteristics with resistance to decay and the emergence of decay

pathways (Dewanckele et al., 2013; Benavente et al., 2007b; Charola, 2000). Differences in the pore-size distribution within single materials have been linked to specific decay patterns as a result of resistance to crystallisation pressures, (Rossi-Manaresi and Tucci, 1991). These can explain the detachment of a surface crust or the emergence of alveolar weathering in heterogeneous stone. Similarly, the presence and distribution of clays in compact stone can result in distinct patterns determined by their structural alignment (Aires-Barros et al., 1998). Pre-existing petrophysical factors can explain the different decay rates and slight divergence in decay patterns observed in the Reigate Stone samples used in this study. Past studies have suggested the relative presence of clays and calcite is likely to be a major control on resistance to decay (Michette et al., 2020; Sanderson and Garner, 2001). Both function as pore filling cement, with calcite also improving strength characteristics and clay improving moisture retention. They are likely to impact differently on the overall shape and heterogeneity of the porous matrix; the rapid decay of GA2_A/B in this study could be linked not only to its weaker, clay bearing matrix, but also to a higher proportion of small pores and higher interconnectivity due to less clogging by calcite. This would place more clay bearing Reigate Stone within the most at-risk category identified by Benavente et al. (2007b). The results of this study clearly indicate that in addition to any hypothesis on environmental control, a hypothesis on material control must be incorporated into models of salt driven decay in Reigate Stone; this confirms observations made on the exterior masonry of the Bell Tower, where powdering and flaking decay patterns correlate to visibly different stone types.

The powdering of stones in the west and north facing elevations of the Bell Tower may be further linked to the formation of an outer crust or casing, which historic photos suggest occurred in response to sulphation in the 19th century. Previous studies have shown that gypsum crust formation depletes calcium ions from the subsurface of calcareous stone (Charola, 2000). When the relatively harder outer layer erodes or detaches, the weakened subsurface is prone to rapid granular disintegration. This decay pathway would explain the presence of alveolars (Bruthans et al., 2018; Mol and Viles, 2012). The underlying mechanics, with capillary migration maintaining a relatively steady state at the exposed surface, could be covered by the hypothesis tested here (Lewin, 1982); a similar process could explain the collapse of sample GA2_B in this study.

The complicating factors in interpreting the results of this study reveal deeper complexities within the current conceptual framework of salt driven masonry decay. Past studies queried the accepted mechanics of Na_2SO_4 driven decay, and the relative role of crystallisation and hydration pressures induced by phase change (Flatt, 2002; Rodriguez-Navarro et al., 2000). This led to greater appreciation of the role supersaturation plays in accelerated ageing experiments. There is still acceptance within the field that salt driven decay is not fully understood (Flatt et al., 2017). Current thermodynamic modelling approaches may be insufficient at fully describing interrelating processes. Even within the framework of existing models, the minute differences and continuous fluctuations between moisture in porous networks and ambient RH can render the predictive capabilities of software such as ECOS imprecise at best (Franzen and Mirwald, 2004).

These issues reflect similar challenges encountered during previous developments of the conceptual framework, some of which were made during a study of Reigate Stone masonry at the Tower of London (Price, 1993; Price, 2007). Parts of the Wakefield Tower were found to be heavily salt contaminated. In an initial study, based on semi-quantitative analysis, Price (1993) tentatively proposed humidity regimes for stabilising the salts present in the masonry. In a later study based on the then newly developed ECOS thermodynamic model, Price (2007) found that the proposed regimes (which had not been implemented) would have been potentially damaging due to unforeseen crystallisation scenarios. In any case, implementing room-scale RH regimes at historic tourist sites has proven highly impractical. Church

(2003) found ambient RH in the Wakefield Tower to lie within the range later predicted to be most damaging in the ECOS model. The most heavily contaminated and rapidly decaying masonry was treated with Brethane in 1984 (Sanderson and Garner, 2001). Inadequate pointing is thought to have contributed to the increased contamination of this south-west lying masonry. The decay rate was shown to have probably increased since treatment. Silanes can increase salt crystallisation pressures in contaminated samples (Ruffolo et al., 2017). This example serves to highlight the complexity of predicting decay and conserving salt contaminated masonry. Even frameworks that account for the thermodynamics of complex salt solutions are of limited value unless they can integrate real world idiosyncrasies such as past treatment history and account for the practicalities of building use.

4. Conclusion

The aim of this paper was to determine the role of environmental conditions on the emergence of decay patterns in Reigate Stone, by simulating typical salt-laden environments which appear to contribute to rapidly decaying Reigate masonry and subject a range of mineralogical typologies to accelerated ageing tests. The focus was on the Bell Tower, which contains Reigate masonry in a range of different environments and of likely different mineralogical typologies, displaying powdering and flaking decay patterns.

Distinct types of complex, mixed salt contaminations are present in different areas of the Bell Tower; however, thermodynamic modelling suggests only two salts are likely to crystallise under ambient conditions. NaCl crystallisation is likely to be occurring in powdering masonry in the lower chamber. In the flaking masonry of the stairwell NaNO_3 crystallisation is likely, with NaCl crystallisation occurring during more pronounced drops. These findings were used to test a hypothesis that powdering is controlled by continuous surface evaporation of saturated masonry at relatively high, stable RH, whilst flaking is controlled by subflorescence in response to a variable moisture profile within the masonry and repeated cycles in RH.

Correlating these crystallisation scenarios with the distinctive patterns of decay observed in the Bell Tower is challenging. There are some indications that the mechanics of decay can be replicated in laboratory conditions. Simulated environment A was characterised by frequent, sharp drops to 60% RH to stimulate NaNO_3 crystallisation, followed by longer periods of 95% RH to stimulate deliquescence and redistribution of the solution. This caused rapid decay of weaker Reigate Stone samples, as well as the detachment of larger flakes in weaker samples or along structural imperfections. This bears some resemblance to the aggressive pattern of flaking decay found in parts of the stairwell. Simulated environment B, designed to mimic powdering in the lower chamber, caused efflorescence when samples were in continuous contact with moisture, and differential rates of loss in response to different RH during drying. This corresponds with phenomena observed in the field. However, viewed in comparison the distinct environments cannot be said to have had a controlling effect on the emergence of decay patterns. Most samples decayed through loss of surface powder, suggestive of near surface crystallisation. Isolated incidents of flake detachment along pre-existing structural imperfections, suggestive of subflorescence, occurred in samples placed in both environments. Widespread subflorescence only occurred in the weakest, most porous sample. Whilst this resulted in immediate surface loss in the aggressive, fluctuating environment A, the response in the stable environment B implied gradual decay beneath a harder surface crust building up to a catastrophic collapse of material. The emergence of distinct decay patterns in response to wetting and drying was therefore governed by stone type and pre-existing structural characteristics, with the specific environmental conditions in this study only affecting the rate of decay.

The implication of these results is that the emergence of decay patterns in Reigate Stone cannot be explained solely by environmental mechanisms; baseline petrology and historical contingency can play a

crucial role. Anamnesis of distinct decay patterns in Reigate Stone masonry can therefore not function as an independent method for diagnosing underlying decay mechanisms and designing conservation strategies based on environmental control. Whilst environmental controls may provide a conservation strategy in some cases, it is likely that detailed assessment of the specific dynamics of salt contamination, environmental parameters and material characteristics will be necessary in every case. With some further development, the methodology presented here should provide an effective contribution to such an assessment.

CRedit authorship contribution statement

Martin Michette: Conceptualization, Methodology, Investigation, Data curation, Formal analysis, Writing – original draft, Visualization. **Heather Viles:** Conceptualization, Methodology, Supervision, Writing – review & editing, Project administration, Funding acquisition. **Constantina Vlachou:** Conceptualization, Supervision, Writing – review & editing, Project administration, Funding acquisition. **Ian Angus:** Conceptualization, Supervision.

Declaration of Competing Interest

The authors declare that they have no known competing financial interests or personal relationships that could have appeared to influence the work reported in this paper.

Acknowledgements

This work was supported by funding from the Engineering and Physical Sciences Research Council (EPSRC) and Historic Royal Palaces (HRP) as a part of the Centre for Doctoral Training in Science and Engineering in Arts, Heritage and Archaeology (SEAHA) [grant number: EP/L016036/1]. The authors would like to thank Mona Edwards from the University of Oxford for technical and analytical support, and two anonymous reviewers for their helpful feedback.

References

- Aires-Barros, L., Basto, M.J., Graça, R.C., Dionísio, A., Rodrigues, J.D., Henriques, F.M. A., Charola, A.E., 1998. Stone deterioration on the tower of Belem/Zerstörung des Natursteins am Turm vom Belem. *Restorat. Build. Monum.* 4 (6), 611–626.
- Amadori, M.L., Lazzarini, L., Massa, S., 1989. Il deterioramento da sodio cloruro di rocce compatte e porose a Venezia. La conservazione dei monumenti nel bacino Mediterraneo. In: 1st International Symposium, pp. 83–89.
- Arnold, A., 1982, July. Rising damp and saline minerals. In: Deterioration and preservation of Stone Objects, Fourth International Congress July 7–9, 1982, Proceedings, pp. 11–28.
- Benavente, D., Cueto, N., Martínez-Martínez, J., García del Cura, M., Cañaveras, A., 2007a. The influence of petrophysical properties on the salt weathering of porous building rocks. *Environ. Geol.* 52 (2), 215–224.
- Benavente, D., Martínez-Martínez, J., Cueto, N., García-Del-Cura, M., 2007b. Salt weathering in dual-porosity building dolostones. *Eng. Geol.* 94 (3), 215–226.
- Bionda, D., 2005. RUNSALT - A Graphical User Interface to the ECOS Thermodynamic Model for the Prediction of the Behaviour of Salt Mixtures under Changing Climate Conditions. <http://science.sdf-eu.org/runsalt/>.
- Bruthans, J., Filippi, M., Slavík, M., Svobodová, E., 2018. Origin of honeycombs: testing the hydraulic and case hardening hypotheses. *Geomorphology* 303, 68–83.
- Burgess, P., 2008. Surrey's Ancient Stone Mines.
- Charola, A.E., 2000. Salts in the deterioration of porous materials: an overview. *J. Am. Inst. Conserv.* 39 (3), 327–343.
- Church, L., 2003. An Investigation into the Deterioration of Reigate Stone at the Wakefield Tower, HM Tower of London. MA dissertation. Institute of Archaeology, University College London.
- Colston, B., Watt, D., Munro, H., 2001. Environmentally-induced stone decay: the cumulative effects of crystallization-hydration cycles on a Lincolnshire oolite-parietal limestone. *J. Cult. Herit.* 2 (4), 297–307.
- Dewanckele, J., Boone, M.A., De Kock, T., De Boever, W., Brabant, L., Boone, M.N., Cnudde, V., 2013. Holistic approach of pre-existing flaws on the decay of two limestones. *Sci. Total Environ.* 447, 403–414.
- Diaz Gonçalves, T., Brito, V., 2014. Alteration kinetics of natural stones due to sodium sulfate crystallization: can reality match experimental simulations? *Environ. Earth Sci.* 72 (6), 1789–1799.
- Eloukabi, H., Sghaier, N., Nasrallah, S.B., Prat, M., 2013. Experimental study of the effect of sodium chloride on drying of porous media: the crusty-patchy efflorescence transition. *Int. J. Heat Mass Transf.* 56 (1–2), 80–93.
- Espinosa-Marzal, R.M., Scherer, G.W., 2013. Impact of in-pore salt crystallization on transport properties. *Environ. Earth Sci.* 69 (8), 2657–2669.
- Flatt, R.J., 2002. Salt damage in porous materials: how high supersaturations are generated. *J. Cryst. Growth* 242 (3–4), 435–454.
- Flatt, R.J., Aly Mohamed, N., Caruso, F., Derluyn, H., Desarnaud, J., Lubelli, B., Shahidzadeh, N., 2017. Predicting salt damage in practice: a theoretical insight into laboratory tests. *RILEM Techn. Lett.* 2, 108–118.
- Franzen, C., Mirwald, P.W., 2004. Moisture content of natural stone: static and dynamic equilibrium with atmospheric humidity. *Environ. Geol.* 46, 391–401.
- Goudie, A.S., 1986. Laboratory simulation of 'the wick effect' in salt weathering of rock. *Earth Surf. Process. Landf.* 11 (3), 275–285.
- Hall, K., Thorn, C., Sumner, P., 2012. On the persistence of 'weathering'. *Geomorphology* 149, 1–10.
- Lewin, S.Z., 1982. The mechanism of masonry decay through crystallization. In: Conservation of Historic Stone Buildings and Monuments. Proceedings of the Conference Held in Washington, DC, February 2–4, 1981, pp. 120–144.
- Liefferink, R.W., Naillon, A., Bonn, D., Prat, M., Shahidzadeh, N., 2018. Single layer porous media with entrapped minerals for microscale studies of multiphase flow. *Lab Chip* 18 (7), 1094–1104.
- Lockwood, S., 1994. Reigate stone: Geology, use and repair. *Struct. Surv.* 12, 18–22.
- López-Arce, P., Doehne, E., Martin, W., Pinchin, S., 2008. Magnesium sulfate salts and historic building materials: experimental simulation of limestone flaking by relative humidity cycling and crystallization of salts. *Mater. Constr.* 58 (289–290), 125–142.
- Lubelli, B., Van Hees, R., Groot, C., 2006. The effect of environmental conditions on sodium chloride damage. *Stud. Conserv.* 51 (1), 41–56.
- Lubelli, B., Cnudde, V., Diaz-Goncalves, T., Franzoni, E., van Hees, R.P., Ioannou, I., Verges-Belmin, V., 2018. Towards a more effective and reliable salt crystallization test for porous building materials: state of the art. *Mater. Struct.* 51 (2), 55.
- McCabe, S., Smith, B.J., McAlister, J.J., Gomez-Heras, M., McAllister, D., Warke, P.A., Basheer, P.A.M., 2013. Changing climate, changing process: implications for salt transportation and weathering within building sandstones in the UK. *Environ. Earth Sci.* 69 (4), 1225–1235.
- Menéndez, B., Petráňová, V., 2016. Effect of mixed vs single brine composition on salt weathering in porous carbonate building stones for different environmental conditions. *Eng. Geol.* 210, 124–139.
- Michette, M., Viles, H., Vlachou, C., Angus, I., 2019. Bellweathered: Reigate Stone decay mechanisms at the Bell Tower, Tower of London. In: Monuments in Monuments 2019 Conference Proceedings, pp. 43–52. <https://pub-prod-sdk.azurewebsites.net/api/file/e99b4f10-3572-4459-a81f-aab00ab0e4e>.
- Michette, M., Viles, H., Vlachou, C., Angus, I., 2020. The Many Faces of Reigate Stone: An Assessment of Inherent Variability in Historic Masonry Based on Medieval London's Principal Freestone Submitted.
- Modestou, S., Theodoridou, M., Ioannou, I., 2015. Micro-destructive mapping of the salt crystallization front in limestone. *Eng. Geol.* 193, 337–347.
- Mol, L., Viles, H.A., 2012. The role of rock surface hardness and internal moisture in tafoni development in sandstone. *Earth Surf. Process. Landf.* 37 (3), 301–314.
- Pel, L., Pishkari, R., Adan, O., 2019, September. Combined wicking and drying of a NaCl solution in porous building materials. In: MATEC Web of Conferences, 282. EDP Sciences, p. 02095.
- Price, C.A., 1993. Preventive conservation of salt-contaminated masonry in the Wakefield Tower, HM Tower of London. *Inst. Archaeol. Bull.* 30, 121–133.
- Price, C.A., 2000. An expert chemical model for determining the environmental conditions needed to prevent salt damage in porous materials. In: European Commission Research Report 11, (Protection and Conservation of European Cultural Heritage). Archetype Publications, London, pp. 1–135.
- Price, C.A., 2007. Predicting environmental conditions to minimise salt damage at the Tower of London: a comparison of two approaches. *Environ. Geol.* 52 (2), 369–374.
- Rodríguez-Navarro, C., Doehne, E., 1999. Salt weathering: influence of evaporation rate, supersaturation and crystallization pattern. *Earth Surf. Proc. Landf. J. Br. Geomorphol. Res. Group* 24 (3), 191–209.
- Rodríguez-Navarro, C., Doehne, E., Sebastian, E., 2000. How does sodium sulfate crystallize? Implications for the decay and testing of building materials. *Cem. Concr. Res.* 30 (10), 1527–1534.
- Rossi-Manaresi, R., Tucci, A., 1991. Pore structure and the disruptive or cementing effect of salt crystallization in various types of stone. *Stud. Conserv.* 36 (1), 53–58.
- Ruffolo, S.A., La Russa, M.F., Ricca, M., Belfiore, C.M., Macchia, A., Comite, V., Pezzino, A., Crisci, G.M., 2017. New insights on the consolidation of salt weathered limestone: the case study of Modica stone. *Bullet. Eng. Geol. Environ.* 76, 11–20.
- Sanderson, R., Garner, K., 2001. Conservation of Reigate stone at Hampton Court Palace and HM Tower of London. *J. Archit. Conserv.* 7 (3), 7–23.
- Sawdy, A., Price, C., 2005a. Salt damage at Cleve Abbey, England: part I: a comparison of theoretical predictions and practical observations. *J. Cult. Herit.* 6 (2), 125–135.
- Sawdy, A., Price, C., 2005b. Salt damage at Cleve Abbey, England. Part II: seasonal variability of salt distribution and implications for sampling strategies. *J. Cult. Herit.* 6 (3), 269–275.
- Sowan, P.W., 1975. Firestone and hearthstone mines in the Upper Greensand of East Surrey. *Proc. Geol. Assoc.* 86 (4), 571–591.
- Sun, Q., Zhang, Y., 2019. Combined effects of salt, cyclic wetting and drying cycles on the physical and mechanical properties of sandstone. *Eng. Geol.* 248, 70–79.
- Veran-Tissoires, S., Prat, M., 2014. Evaporation of a sodium chloride solution from a saturated porous medium with efflorescence formation. *J. Fluid Mech.* 749, 701–749.

Vergès-Belmin, V., 2008. Illustrated Glossary on Stone Deterioration Patterns. ICOMOS.
Warke, P., Smith, B., 2007. Complex weathering effects on durability characteristics of building stone. *Geol. Soc. Lond., Spec. Publ.* 271 (1), 211–224.

Yu, S., Oguchi, C.T., 2009. Complex relationships between salt type and rock properties in a durability experiment of multiple salt–rock treatments. *Earth Surf. Process. Landf.* 34 (15), 2096–2110.